Rainfall over the Tropical Western Pacific in relation to SST and mesoscale gradients thereof

Yanping Li[1] and R. E. Carbone[1,2]

[1]International Pacific Research Center and Department of Meteorology, University of Hawaii at Manoa, 2525 Correa Road, Honolulu, HI, 96822

[2]National Center for Atmospheric Research,Boulder, CO
P.O.Box 3000, Boulder, CO, 80307-3000

Introduction:

We have examined 4-year of satellite-derived SST (GHRSST) and rainfall data (CMORPH) in anticipation of a relationship between SST structure and the excitation of convective rainfall. Rainfall distribution and event Regimes are discussed, followed by the study of SST morphology and lower boundary forcing.

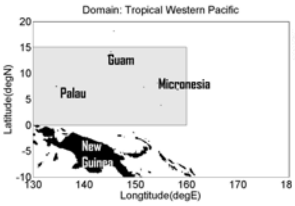

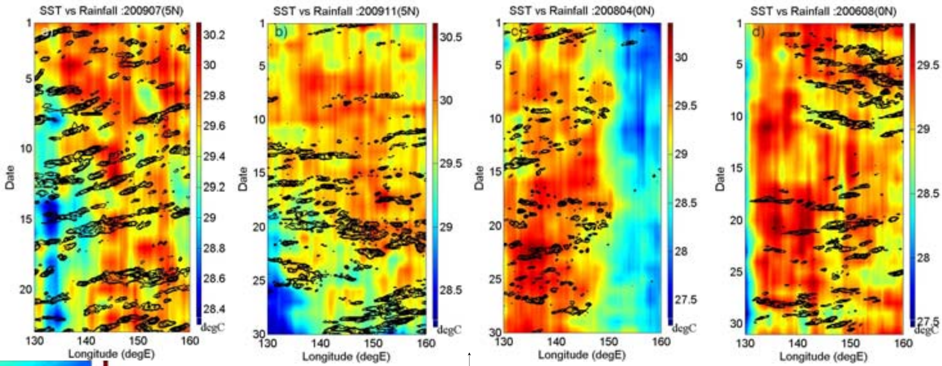

Figure 2: Hovmöller diagrams of characteristic monthly periods at 5N and EQ. SST in background; contoured precipitation events. Precipitation regimes include westward propagating, local diurnal, eastward propagating and suppressed conditions.

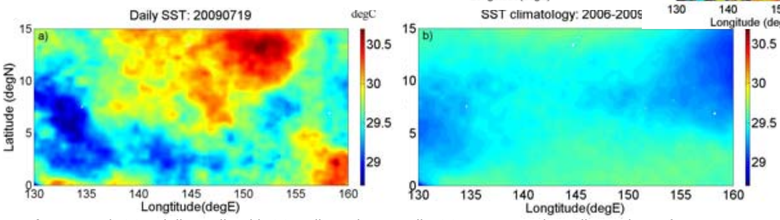

Figure 1: a) SST daily reality, b) SST climatology. Daily SST areas and gradients thereof are multi-scale and extend over a larger dynamic range.

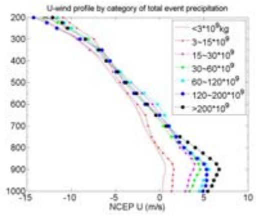

Figure 3: U-wind profile as stratified by categories of total precipitation per event (kg). Systematic precipitation increase is associated with an increase in shear, which is mainly associated with increasing lower tropospheric westerly flow (Sep 2009).

SST morphology and lower boundary forcing

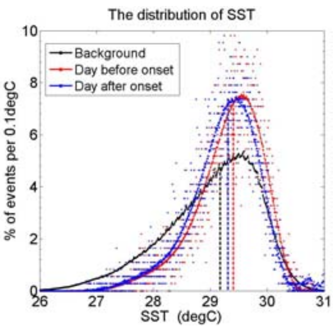

Figure 5: 4-year distribution of rainfall- onset SST and background SST. Mean onset-SST is slightly higher than background mean. Overall, onset occurrence is disproportionately concentrated in mid-SST range. The warmest SST areas are neutral with respect to frequency of onset.

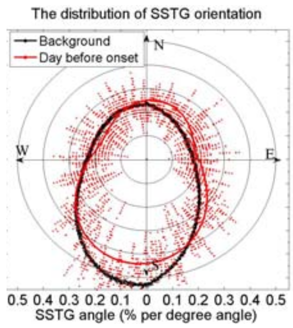

Figure 6: 4-year background SST orientation distribution (black); onset orientation distribution (red). Phase change suggests onset is less favored at southward-pointing SSTG and preferred at eastward-pointing SSTG (west side of warm anomaly in westerly flow).

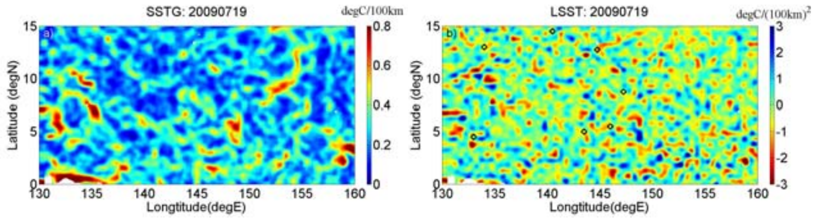

Figure 4: a) Multi-scale variation of large amplitude SST gradient field, cellular structure throughout and mesoscale structure on the large scale gradient. b) Examples of –LSST field and precipitation onset locations. Symbols illustrate precipitation onset locations. Positive values connote likely locations of enhanced atmospheric horizontal convergence near lower boundary.

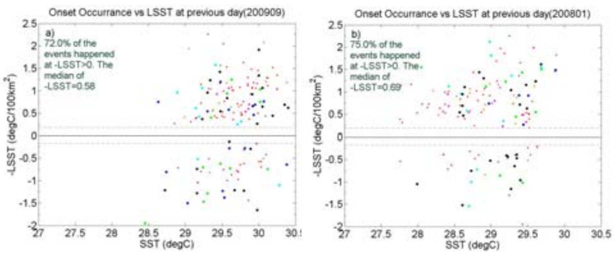

Figure 7: Distributions of rainfall onset in relation to -LSST and SST for a) Sep 2009, b) Jan 2008. The dash lines near zero -LSST are 3 σ uncertainty of background convergence (converted to LSST unit) about zero. -LSST values plotted are the largest absolute value, conserving sign of the local area average within GHRSST (microwave) footprint.

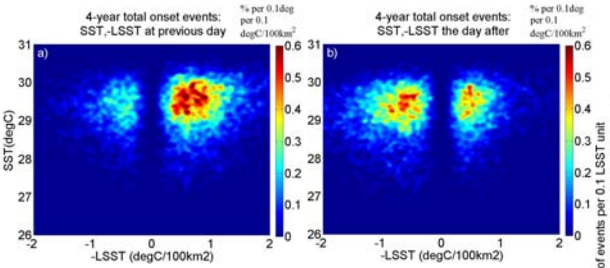

Figure 8: SST, -LSST distribution before and after onset events: (a) previous day (b) following day. As expected, there is a large shift from convergent to divergent curvature of -LSST at 29-29.5°C SST.

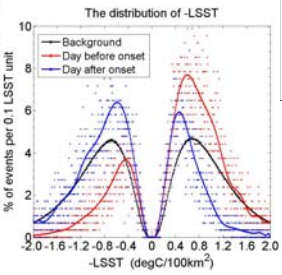

Figure 9: The before-after onset shift in relation to background -LSST. The shift represents approximately a factor of two from background frequency in each phase.

Polynomial curve fit method:

$$SST(x_0,y)\approx D_p(y-y_0)^p+\cdots D_2(y-y_0)^2++D_1(y-y_0)^1+D_0$$

$$SST(x_0,y)\approx D_p(y-y_0)^p+\cdots D_2(y-y_0)^2++D_1(y-y_0)^1+D_0$$

SSTG: $\left.\frac{\partial SST(x,y_0)}{\partial x}\right|_{x=x_0}+\left.\frac{\partial SST(x_0,y)}{\partial y}\right|_{y=y_0}=C_1+iD_1$

LSST: $\left.\frac{\partial^2 SST(x,y_0)}{\partial x^2}\right|_{x=x_0}+\left.\frac{\partial^2 SST(x_0,y)}{\partial y^2}\right|_{y=y_0}=2(C_2+D_2)$

Estimation of -LSST derived local convergence

Gravity wave Approximation:

$$-(u_x+v_y)_t=w_{zt}=p'_{xx}+p'_{yy}=$$

$$-\frac{\bar{\rho}_b gH}{\bar{T}_b}(T'_{xx}+T'_{yy})=-\frac{\bar{\rho}_b gH}{\bar{T}_b}\cdot LSST$$

so $-(u_x+v_y)=w_z=-\frac{\bar{\rho}_b gH}{\bar{T}_b}\cdot LSST_m\cdot\Delta t$

Assume PBL height H=350m, $-LSST_m$~ 0.6°C/100km^2, Δt=54000s,

$$con\sim\frac{9.8\times 350}{300}\cdot\frac{0.6}{(10^5)^2}\cdot 54000\approx 4\times 10^{-5}\ s^{-1}$$

Background convergence:

w at 925 hPa is ~ $2\times 10^{-3}\ m\cdot s^{-1}$
PBL height H=750m,
Mean $con\sim 3\times 10^{-6}\ s^{-1}$

Gravity current Approximation:

Assume PBL height H=350m, horizontal scale 50km, temperature difference drops 50% at PBL top, $\Delta T\sim 0.3^oC$

$$v=\sqrt{kgH\frac{\Delta T}{T}}\sim\sqrt{1\times 9.8\times 350\times\frac{0.3}{300}}=1.8\,ms^{-1}$$

For 3-d cyclinder symmetric shape,

$$con=\frac{\partial v}{\partial x}=\frac{1}{A}\cdot\frac{\partial A}{\partial R}=\frac{1}{\pi R^2}\cdot 2\pi R=\frac{2v}{R}=7\times 10^{-5}\ s^{-1}$$

assume that real density current propagated at ~0.5 average speed of a "free" density current

$$convergence\sim 3.5\times 10^{-5}\ s^{-1}$$

Acknowledgement:

This research is supported by NOAA sponsorship of the International Pacific Research Center (IPRC), University of Hawaii; NCAR is supported by the National Science Foundation.

Conclusion:

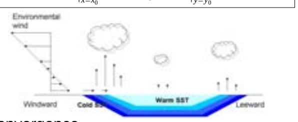

1. Approximately 75% of rainfall events are spatially and temporally coincident with a maximum of surface convergence (-LSSTmax).

2. The Laplacian derived local convergence is ~10^{-5} s^{-1}, one order of magnitude larger than regional background convergence.

3. SST structure reveal a high time rate of change in patches of order 100km dimension. Warm oceanic anomalies can turn cold in one day, likely to be the consequence of convectively generated winds and precipitation.

4. Onset orientation occurs preferentially at eastward-directed SSTG. In westerly flow, this indicates a preference for onset of rainfall on the windward (western) side of a warm patch.

5. In regimes associated with moderate wind shear and a lower-tropospheric critical level, heavy precipitation from long-lived propagating systems is common (up to 4 days, 2000 km).

Future work:

1. Investigate the potential for coherent amplification effects that could arise from propagating mesoscale convective systems that are dynamically coupled to evolving SST gradient zones. A "dance" of this type might also influence the amplification or dissipation of larger scale tropical free waves, such as inertial gravity waves, mixed Rossby waves, or Kelvin waves.

2. Seek to obtain a more complete understanding of local diurnal convection (i.e. non-propagating) and coupled ocean-atmosphere cycles more generally. The oceanic capacity to accumulate daily residuals of energy, leading to periodic cycles of convective rainfall, may point toward an intrinsic time scale for accumulation of SST gradients .

Reference: Yanping Li, R. E. Carbone, 2011: Excitation of rainfall over the tropical western Pacific. *Submitted to JAS.*